

Characterization of anodized and bare 7075-T6 aluminum alloy treated with Zr-based conversion coating

Jéssica Salles Pinheiro ^{1*} 

Claudia Trindade Oliveira ²

Gabriel Regio ³

Nicolle Goi ⁴

Jane Zoppas Ferreira ¹

Abstract

AA7075-T6 is an aluminum alloy that has a high mechanical resistance; however, it shows corrosion vulnerability. A usual method to improve the corrosion resistance is anodization in acidic medium, which forms a thin barrier layer and a thicker porous oxide layer over the surface. This ultimate layer must be sealed to avoid electrolyte penetration. In the present work, a Zr-based conversion coating was investigated as a novel method of cold sealing and compared to the precipitation over bare AA7075-T6. The samples were characterized by Scanning Electron Microscopy (SEM) and Energy Dispersive X-Ray Spectroscopy (EDX) to elucidate the mechanism of reaction on both natural aluminum oxide and anodic oxide layer. The hydrophobicity properties were evaluated by contact angle measurements. The mechanism of deposition suggested for the coating over the anodic oxide was analogue to the one that takes place over the bare alloy: an initial attack by fluoride ions, local pH increase and Zr oxide precipitation. It was also possible to precipitate Zr oxide inside the pores. An increase of 125% on the contact angle was observed for the Zr coating over anodized surfaces, while the increase over the bare alloy was of 32%. Therefore, a robust coating system can be proposed involving the anodic layer and the nanometric Zr oxide.

Keywords: Aluminum alloy; Anodizing; Conversion coating; Hydrophobicity.

1 Introduction

It is well known that aluminum alloys from 7000 series are widely used to structural purposes, since they present high tensile strength, as well as fatigue and abrasion resistance and are also lighter than any steel alloy. This last property being of great interest mainly for aeronautical industry [1]. Among these alloys, AA7075 is one of the most used, often hardened by a heat treatment of artificial ageing, called T6. Through this procedure, second phase elements are added to ensure a higher hardness. For the AA7075-T6 the main elements added are Zn and Mg, but Fe, Si, Cu and Mn are also present [2-5]. However, these particles are responsible for a major vulnerability of the material to localized corrosion since they form intermetallic particles that act as galvanic micro-cells – 80% of these particles are cathodic or tend to become cathodic in relation to aluminum, causing the vicinities of each particle to corrode preferably [4,5]. Facing this limitation, a suitable surface protection is required to this material. One of the possibilities to protect aluminum

alloys from corrosion are chromium-based coatings, which can provide high corrosion resistance, but it should be considered that those which perform the better are the worst in terms of toxicity issues: coatings containing Cr(VI) ions are proven to be toxic to both humans and the environment and are already prohibited in great part of the world [6,7].

On the other hand, there are non-toxic methods that are already used. One of those is the conversion coating based on H_2ZrF_6 solutions, which can be easily applied rather by spraying or immersion, providing a nanometric oxide layer capable of increase corrosion protection and adhesion to painting and other organic coatings [8]. Besides, there is another conversion coating that shows great performance and is widely used in aerospace industry, which consists in anodization. The most common way of anodizing is performed in acidic medium, where a porous layer of alumina is obtained while an amount of current or potential is applied. Mixtures of inorganic and organic acids are being used as

¹Laboratório de Corrosão, Proteção e Reciclagem de Materiais – LACOR, Programa de Pós-graduação em Engenharia de Minas, Metalúrgica e de Materiais – PPGE3M, Universidade Federal do Rio Grande do Sul – UFRGS, Porto Alegre, RS, Brasil.

²Instituto de Ciências Exatas e Tecnológicas, Universidade Feevale, Novo Hamburgo, RS, Brasil.

³Departamento de Engenharia de Materiais, Universidade Federal do Rio Grande do Sul – UFRGS, Porto Alegre, RS, Brasil.

⁴Laboratório de Corrosão, Proteção e Reciclagem de Materiais – LACOR, Universidade Federal do Rio Grande do Sul – UFRGS, Porto Alegre, RS, Brasil.

*Corresponding author: jessica.salles@ufrgs.br



electrolyte in order to replace chromic acid and thus comply with the requirements of aerospace industry and also being environmentally correct [9-12]. To ensure the protection capacity of this coating, the porous characteristic must be eliminated, i.e., the pores must be sealed in order to avoid the penetration of corrosive electrolyte towards the metal surface [13]. This means that the porous net could also work as a rougher surface that would anchor other types of coating, and thus enable an extra resistance [14].

The most common sealing technique used by the industry is thermal sealing, where a hydroxide is formed through the hydration of alumina, plugging the pores until corrosion protection is improved. Nevertheless, this protection improvement sometimes is not sufficient, so for a long time Cr(VI) solutions were used to achieve better results, because of its high capacity of corrosion protection and self-healing [6]. But as it was already mentioned, Cr(VI)-based surface treatments are being banned from industrial methodology, so a field of research is open, aiming to find non-toxic post-treatments for these anodized aluminum alloys that can provide high corrosion resistance.

Traditional sealing methods spent high energy amounts (temperatures up from 90 °C), therefore other methods are being studied aiming to successfully seal the pores at room temperature and that are also chromium-free. Most studies of novel sealing methods have reported lower corrosion resistance for cold sealing methods than for hot sealing solutions – even when it is only boiling water [9,15]. There were studies of processes carried out at 50 °C [16], 70 °C [17], or both complex and high temperature processes, i.e., sol-gel coatings [18-20]. However, there were some promising methods, where it was possible to improve the corrosion resistance using lower temperatures [21,22]. One of those promising recent studies has shown that a Zr-based conversion coating can be used as a protection to porous layers produced by anodizing in TSA of the AA7075-T6 alloy, at room temperature, enhancing its corrosion resistance more than hydrothermal sealing [21].

This study aims to analyze the Zr-based conversion coating as a post-treatment for the AA7075-T6 alloy, applied by immersion at room temperature, after anodizing in tartaric-sulfuric acid, comparing its morphology to that of samples with and without sealing. Also, a comparison of the same coating applied over the non-anodized alloy was performed, to comprehend the similarities and possible differences between both oxides – natural and anodic alumina – as substrates for the Zr oxide precipitation. In order to do so, SEM, EDS and contact angle analyses were performed to evaluate the surface properties of the different protection systems.

2 Materials and methods

The samples used for the present work consisted of AA7075-T6 aluminum alloy plates with 80 mm high, 40 mm wide and 2.8 mm thick. Table 1 shows the composition of the plates, measured by X-Ray Fluorescence.

The XRF results are not totally in accordance with the nominal composition of the AA7075-T6 alloy. The Cu amount was lower than expected, i.e., 1.2% to 2% [23]. Since Cu is responsible for most of the problematic intermetallic particles in terms of anodizing [23-27], its lower amount might have caused a positive outcome on the anodic film formation of this study.

2.1 Preparation of samples for anodizing

The samples were sanded with SiC papers from #320 up to #4000 and then polished with diamond paste of 1 µm. Then, degreasing was performed using Saloclean 667N from Klintex® (a neutral degreaser made for Al and its alloys, containing sodium carbonate, sodium metasilicate and nonyl ethoxylated phenol) 70 g.L⁻¹ at 70 °C for 10 min. After that the samples were rinsed with deionized water and dried with hot air jet prior to the pickling process, which was an immersion in NaOH 10% (wt.) for 2 min followed by deoxidation/neutralization and removal of some precipitates from the surface immersing the samples in HNO₃ 30% (v.) for 30 s, both at room temperature. After these processes the samples were rinsed with deionized water and dried with hot air jet a last time before each coating procedure to which they were subjected.

2.2 Anodizing process

A mixture of an inorganic and an organic acid was used as the electrolyte for the anodizing process. The solution called TSA is compound by sulfuric acid and tartaric acid in proportions of 40 g.L⁻¹ H₂SO₄ + 80 g.L⁻¹ C₄H₆O₆. Also, a commercial surfactant, Arkopal® (4-nonylphenyl-polyethylene glycol) from Sigma-Aldrich, 1 g.L⁻¹, was added to the electrolyte to ensure the cathodes wettability and thus ensure the current flow during the anodizing processes [18,28]. The cathodes were two Pb leaves of 10 cm wide and 6 cm high each, one in front of the other inside the anodizing cell, separated by 14 cm. At the center, the samples were arranged so as to be equidistant from both cathodes, attached to a copper wire by metal fasteners, ensuring adequate electrical contact. The anodizing process was galvanostatic and the current was provided by a source of the model iCEL PS-5000,

Table 1. Chemical composition (% wt.) of the aluminum alloy used in this work

Al	Zn	Mg	Fe	Si
92.096 ± 0.229	5.712 ± 0.062	1.222 ± 0.278	0.291 ± 0.016	0.116 ± 0.023
Cu	Zr	Ti	Mn	Cr
0.154 ± 0.007	0.088 ± 0.002	0.052 ± 0.005	0.046 ± 0.012	0.206 ± 0.007

applying a current density of $1 \text{ A}\cdot\text{dm}^{-2}$ for 20 min. The process was carried out under constant agitation using a magnetic bar at a constant temperature of $20 \text{ }^\circ\text{C}$ [29]. Temperature control was achieved through a thermostatic bath connected to glass coils placed inside the anodizing cell. The samples had a working area of 25 cm^2 on each side. Subsequently, the anodized samples were rinsed with deionized water inside a beaker and under agitation for 1 min to remove excess acid from the pores and then dried with warm air jet.

2.3 Thermal sealing process

In order to hydrothermally seal the pores of anodized samples, immersions were made in boiling deionized water for 20 min. This time of sealing was chosen based on the literature [30], considering the thickness of the obtained anodic oxides and adding 2 min to ensure a suitable sealing.

2.4 Zr Conversion coating

The conversion coating was produced from hexafluorozirconic acid (H_2ZrF_6) aqueous solutions. These solutions were prepared from a 50% (wt.) commercial solution from Sigma-Aldrich, which density is $1.512 \text{ g}\cdot\text{mL}^{-1}$. The final concentration was $15 \text{ g}\cdot\text{L}^{-1}$ of H_2ZrF_6 , and the pH was adjusted to 3 and 3.5, using a solution of NaOH $40 \text{ g}\cdot\text{L}^{-1}$. A Marconi MA765 disc lift was used to perform the dip-coating method. The time of immersion was maintained at 2 min and the rate for both immersion and removal at $420 \text{ mm}\cdot\text{min}^{-1}$. The processes were carried out at room temperature – between $20 \text{ }^\circ\text{C}$ and $25 \text{ }^\circ\text{C}$. Subsequently, the samples were rinsed with deionized water and dried with

warm air jet. This procedure was carried out to both bare and anodized alloys.

2.5 Characterization of anodized layer and conversion coating

All the samples were characterized by Scanning Electron Microscopy (SEM) and Energy Dispersive X-Ray Spectroscopy (EDX), using a Phenom ProX equipment, under an acceleration voltage of 15 kV for SEM images and 5 kV for EDX measures. In order to verify the hydrophobicity of each surface, contact angle measurements were performed. The assay was performed by the sessile drop method using a SEO Phoenix Mini equipment and the liquid used was ultrapure water. The contact angle of each drop was determined by an image analysis program and averages were obtained from at least 5 measurements for each sample.

3 Results

3.1 Scanning Electron Microscopy (SEM) and Energy Dispersion X-ray Spectroscopy (EDS)

3.1.1 Post-treated bare samples

The surface of the AA7075 alloy without anodizing that was treated with Zr conversion coating is shown in Figure 1. The chemical analyses are present in Table 2. Region 1 comprises the scan of the whole analyzed area, while on the zoomed area the measures were performed in points. Point 2 showed a cathodic particle, near to which a high amount of white precipitate was formed. Point 3 showed

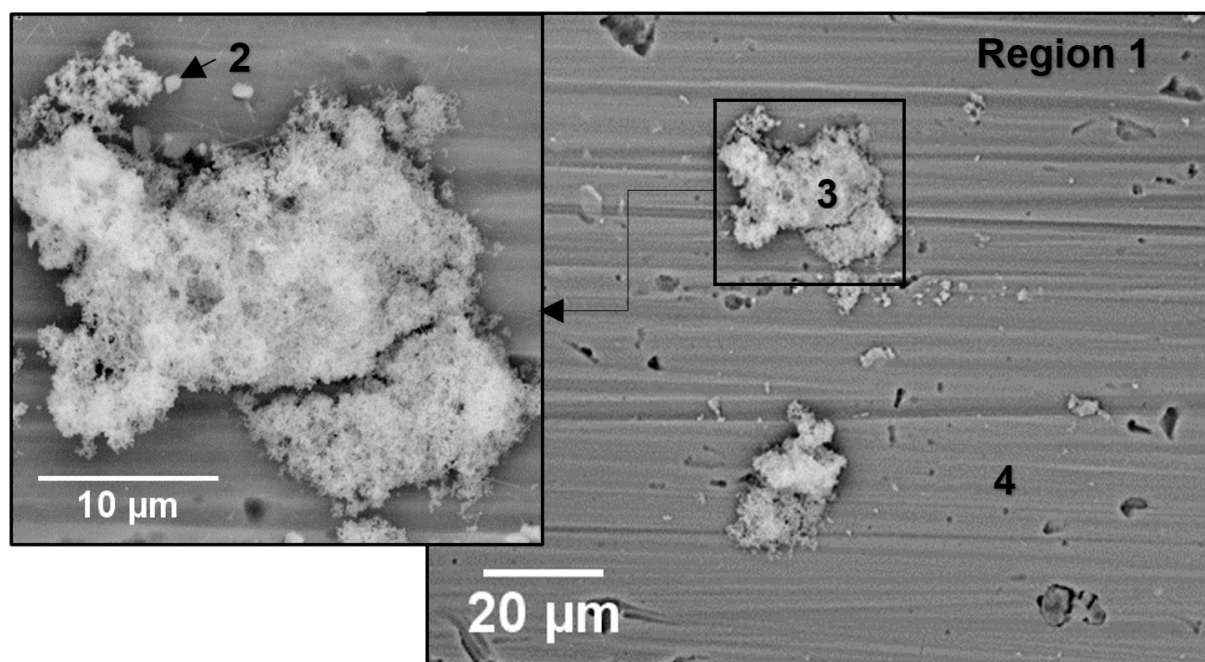


Figure 1. SEM micrograph of the bare AA7075 alloy treated with H_2ZrF_6 .

Table 2. Chemical compositions (%wt.) of region 1 and points 2 to 4 in Figure 1

	Zr	O	Al	F	Zn	Mg	Fe	Si
1	5.35	5.85	79.43	1.84	5.77	1.76	-	-
2	8.69	7.10	67.53	6.04	3.54	1.25	5.84	-
3	35.87	16.79	34.84	8.50	3.27	0.73	-	-
4	4.39	4.80	81.08	1.89	5.80	2.04	-	-

the highest concentration of Zr, indicating that this white morphology found in abundance consists of precipitation of Zr oxide

3.2 Post-treated anodized samples

The SEM micrographs of the surfaces of AA7075 anodized in TSA are shown in Figure 2. Figure 3 and Tables 3 to 5 present the analyzed regions and their respective mass compositions. Region 1 corresponds to the analysis of the entire region of the image, performed by scanning.

Figure 4 shows the SEM images of the cross section of AA7075 alloy anodized and covered with the nanometric Zr coating.

3.3 Contact angle analysis

The sessile drop over the AA7075 surface after treatment with H_2ZrF_6 and the results obtained for the same treatment over the anodized layer are shown in Figure 5.

4 Discussion

4.1 Post-treated bare samples

The morphology after immersion in H_2ZrF_6 presented several regions with white irregular depositions. The chemical analyses (Table 2) indicated a preferential deposition of Zr on the regions with precipitates, which agrees with the literature [7,8,31]. Higher amounts of white precipitate were formed near to cathodic particles (point 2 of EDS analysis). That corroborates with the literature regarding the cathodic particles increasing the activity of the Al matrix around them and thus promoting a greater deposition of the conversion layer [8,32]. In addition, a high content of Zr and fluoride was detected, which suggests that the F^- ions present in H_2ZrF_6 solution play an important role on the deposition of the Zr conversion layer. That proposition is also in agreement with the literature [9,33,34].

4.2 Post-treated anodized samples

The SEM images of the surfaces of AA7075 anodized in TSA revealed a heterogeneous oxide with irregular porosity, containing second phase particles that were not anodized, some of those are indicated by red arrows on Figure 2a, as García-Rubio et al. [35] had found for AA2024 alloy anodized in TSA. One can observe that the anodized samples

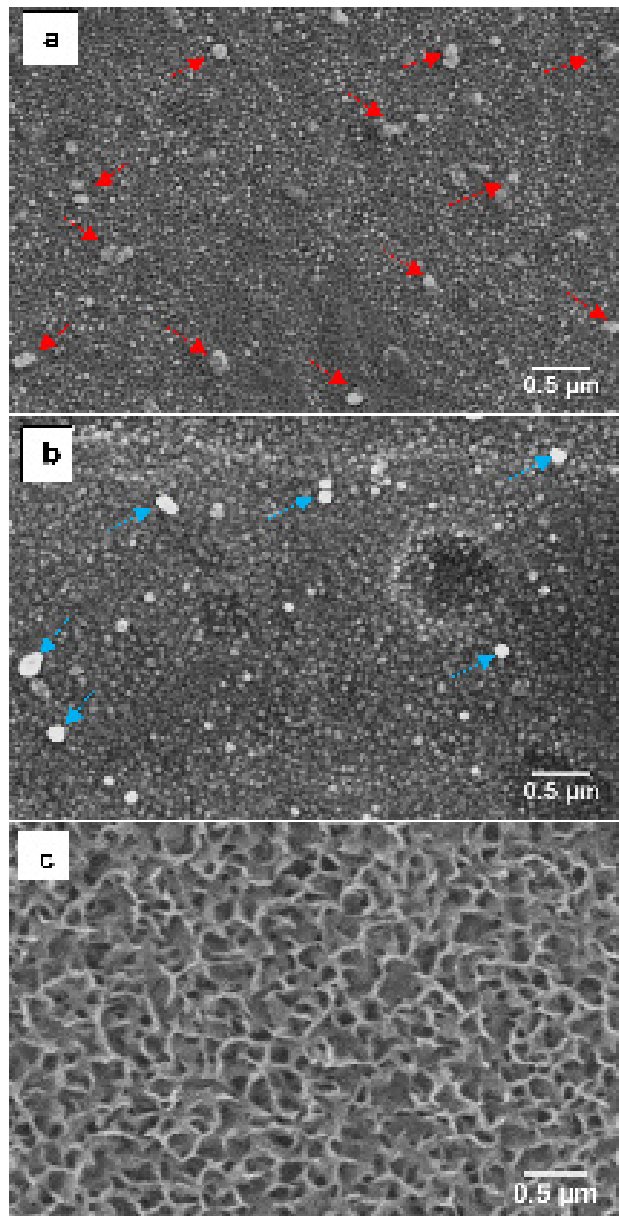


Figure 2. SEM micrographs of AA7075 alloy anodized in TSA without sealing (a), after immersion in H_2ZrF_6 1% (pH 3) (b) and with thermal sealing (c).

treated with H_2ZrF_6 were not drastically modified: only a slightly coarser porosity was observed (Figure 2b), which was comparable to what was found for the AA2024 anodized in TSA and post-treated with Alodine® 1200 – conversion coating based on Cr(VI) [35] and is in agreement with the initial attack promoted by the F^- ions. In addition, regions with

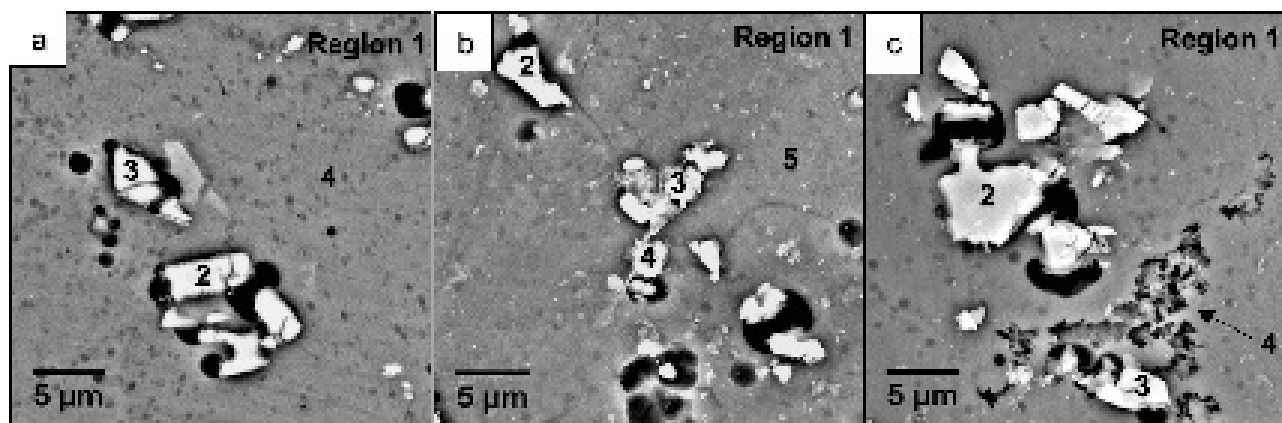


Figure 3. SEM micrographs of anodized AA7075 alloy without sealing (a), immersed in H_2ZrF_6 1% solution with pH 3 (b) and 3.5 (c), indicating the points where EDS analyses were performed.

Table 3. Chemical compositions (%wt.) of the region (1) and points 2 to 4 in Figure 3a

	O	Al	Zn	Mg	Fe	Si	S
1	49.64	44.39	2.31	0.38	-	-	3.28
2	40.63	43.96	1.09	-	10.29	2.24	1.79
3	43.01	44.26	1.09	-	7.40	1.92	2.33
4	49.15	43.71	3.16	0.53	-	-	3.45

Table 4. Chemical compositions (%wt.) of the region (1) and points 2 to 5 of Figure 3b

	Zr	O	Al	F	Zn	Mg	Fe	Si	S
1	6.34	42.27	41.89	2.17	3.91	0.27	-	-	3.16
2	12.86	31.15	36.75	6.11	1.97	-	7.75	1.88	1.53
3	17.07	34.20	36.83	3.40	2.89	-	2.27	0.85	2.49
4	6.48	26.08	45.95	6.33	2.36	0.29	9.13	1.48	1.90
5	4.61	44.23	43.21	-	4.52	-	-	-	3.42

Table 5. Chemical compositions (%wt.) of the region (1) and points 2 to 5 of Figure 3c

	Zr	O	Al	F	Zn	Mg	Fe	Si	S
1	9.38	42.56	38.85	2.46	4.04	-	-	-	2.71
2	21.39	32.88	28.42	5.73	2.08	-	6.71	1.23	1.56
3	20.60	38.94	22.59	10.52	2.37	-	2.15	1.20	1.64
4	12.72	37.83	39.28	3.73	4.22	-	-	-	2.21
5	6.68	43.13	43.22	-	3.15	0.59	-	-	3.24

clear precipitates were observed and subsequently identified as the conversion coating upon the cathodic particles of the alloy, indicated by blue arrows on Figure 2b. In contrast, for the sample that underwent hydrothermal sealing, a considerable morphological alteration was observed, showing typical crystals in “petal” shape across the surface (Figure 2c), which indicates a successful sealing [36].

As it was possible to evaluate by EDS chemical analyses, all samples of AA7075 anodized in TSA presented oxygen content, which was expected due to the formation of alumina. A certain amount of remanent sulfur was also verified, incorporated from the anodizing bath, which was also expected and already described in literature [12,15,17]. It was possible to detect the presence of Zr on the samples treated with H_2ZrF_6 as is was already described in previous works [21,37].

More precipitates with slightly larger sizes were visible on the entire surface treated with H_2ZrF_6 (Figure 2b), which is consistent with the precipitation of Zr oxide on and around the cathodic particles that were not anodized and remained on the surface, according to the chemical analyses (Table 2) and with the literature for non-anodized [8,32] and for anodized aluminum alloy [21,37]. Therefore, one can consider that the phenomenon observed after the treatment with H_2ZrF_6 of AA7075 on non-anodized alloys occurred in an analogue way for the anodized alloy.

The H_2ZrF_6 solution with pH 3.5 promoted a more effective precipitation of Zr oxide than that with pH 3, according to the contents obtained for Zr on both points on the intermetallic particle (points 2 and 3 of Table 5, comparing to the same points of Table 4). The important role of F anions on the deposition mechanism was evidenced,

since the EDS analysis at the oxide layer showed no amount of F and, consequently, less content of Zr (point 5 of both Tables 4 and 5), in contrast to what happens near to cathodic particles.

Previous studies have demonstrated the efficacy in terms of corrosion resistance of these treatments for anodized AA7075 alloy [21,37]. That improvement of corrosion resistance was attributed to a sealing behavior of the conversion coating when applied to the anodic layer, verified by Electrochemical Impedance Spectroscopy (EIS) measures, and compared to hydrothermal sealing. A model of Electrical Equivalent Circuit (EEC) was proposed, suggesting that the nanometric ZrO_2 can penetrate into the porous layer, leading to a partial sealing of the pores [21,37]. The SEM micrographs of cross section samples (Figure 4) showed no increase of thickness when they were immersed in H_2ZrF_6 solution, which supports the hypothesis of that nanometric Zr oxide particles could react with the outer porous layer, growing (i.e., precipitating) towards its interior. Aiming to a complete understanding of the interaction between the nanometric oxide with the anodic oxide, this system should be further investigated by TEM analysis, as was done by George et al. for Zr-based conversion coatings on aluminum and Al-Cu alloys [38]. Notably, these authors verified a process that comprised simultaneously the natural oxide consuming and the Zr oxide growing, focusing on the influence of immersion time and Cu presence on the rate of Zr oxide growing.

4.3 Contact angle analysis

The analysis of the contact angle for the different protection systems of AA7075 alloy revealed different surface properties for each of them. Treatments of chemical modification of the surface aiming to increase the contact angle of aluminum alloys were performed by Liu et al. [39]

on anodized layers, but not involving Zr conversion coating, and by Thangavelu et al. [40], whose study comprised nanocomposite coatings containing ZrO_2 over AA7075, but without anodization. After anodizing in tartaric-sulfuric acid, a hydrophilic surface was verified, which is consistent with the literature [41]. An increase of 32% in the contact angle after the treatment with H_2ZrF_6 was observed (Figure 5). Some increase was already expected, since this treatment results in the deposition of nanometric oxides and obtaining nanometric morphologies is one of the possible ways to form hydrophobic and superhydrophobic surfaces [42-45]. The same treatment over the anodized layer promoted a more pronounced effect on contact angle: an increasing of 123% (for pH 3) and 127% (for pH 3.5). Moreover, the samples that were not anodized showed greater dispersion in the results, which suggests a greater heterogeneity of the coating – this hypothesis is in accordance with the SEM results, that showed an accumulation of Zr oxide close to cathodic particles and other areas with very lower amount of Zr (Figure 1 and Table 2).

A difference between both substrates was expected because of the nature of anodized layers, that is, rougher than the natural aluminum oxide. A surface full of pores that result in a larger area for the reaction of Zr oxide precipitation to take place. Thus, the anodized layer acted as the first step to obtain hydrophobic surfaces – increase the roughness, i.e., geometrically increases hydrophobicity, according to Wenzel's model [42] – while the Zr nanocoating represented the second step – the chemical modification, leading to an increase on the amount of air trapped within the pores, accordingly to Cassie model [41,43,44]. That is, since the Zr oxide can precipitate inside and over a large amount of pore mouths from the outer porous layer, acting as an appropriate sealing method [21,37], a most dense and homogeneous conversion coating is formed, and this becomes a more robust system, suitable to achieve hydrophobicity.

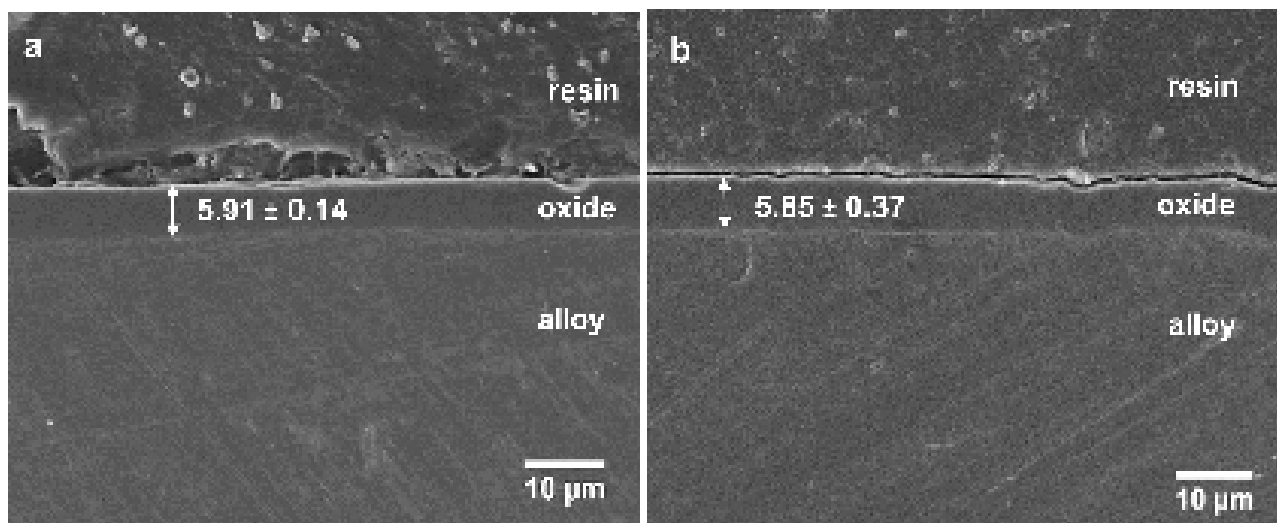


Figure 4. SEM images of the cross sections of samples of the AA7075 alloy anodized in TSA: unsealed (a) and treated with H_2ZrF_6 1% solution (pH 3.5) (b), with their respective thickness values and standard deviations.

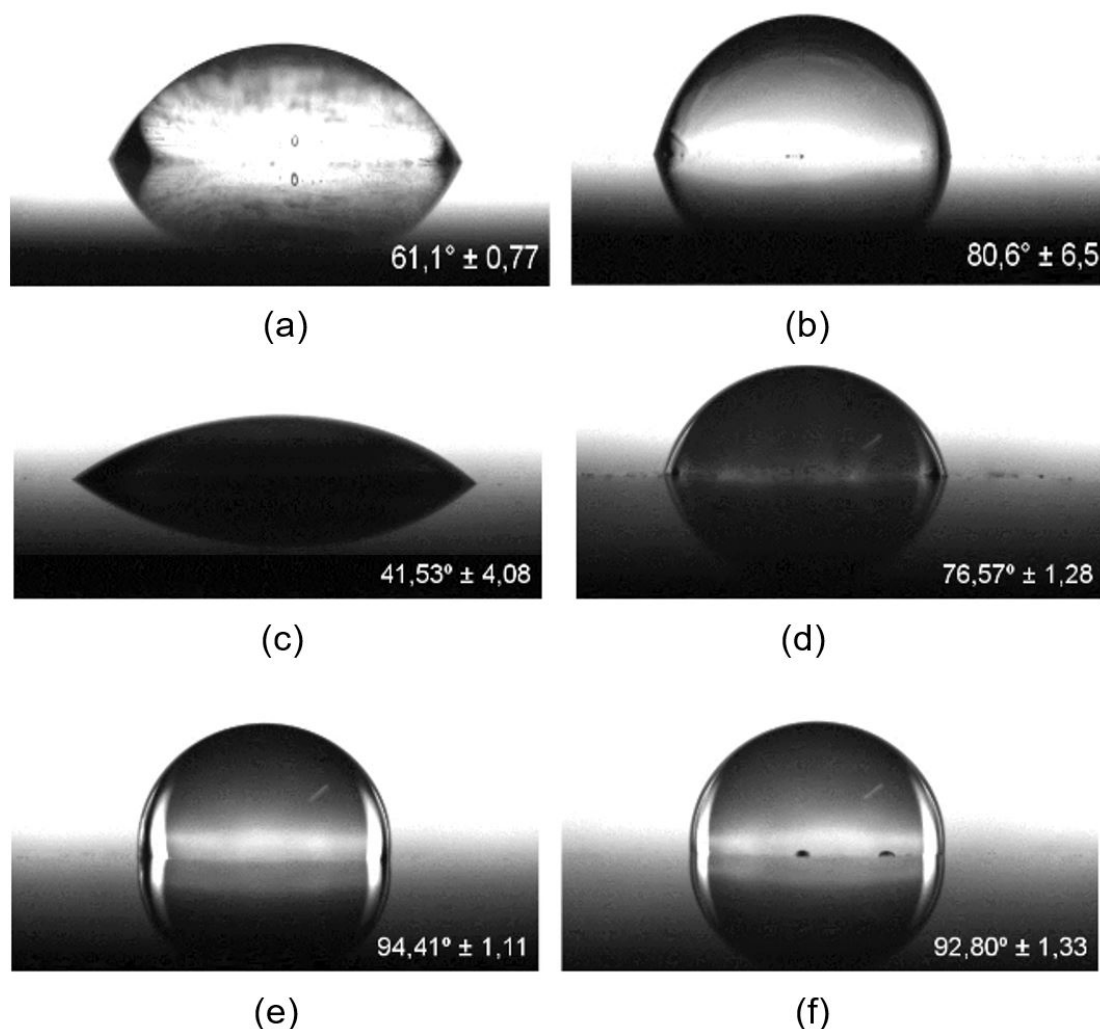


Figure 5. Sessile drop images obtained for the AA7075 alloy surfaces: bare (a), treated with H_2ZrF_6 1% solution pH 3.5 (b) and anodized in TSA (c-f): unsealed (c), hydrothermally sealed (d), treated with H_2ZrF_6 1% solution (e, f): pH 3.0 (e) and pH 3.5 (f).

For the anodized samples that were post-treated with H_2ZrF_6 (Figure 5e, 5f), a hydrophobic behavior was verified, that is, a contact angle greater than 90° , indicating that Zr oxide causes a change in the surface properties of the anodized layer of the AA7075 alloy, which was hydrophilic before the treatment. Although the results of microscopy showed a slight difference between samples treated with solutions of pH 3 or 3.5, the surface properties evidenced by contact angle for both treatments of pH 3 or 3.5 were considered the same, i.e., the difference stayed within the standard deviation. A wider range of pH values should be investigated to verify their influence on the contact angle.

The hydrothermally sealed anodized surface showed a contact angle of 76.5, that is, an increasing of 84% compared to unsealed one, which means it provided a lower increase on the contact angle compared to the post-treatment with H_2ZrF_6 , not reaching hydrophobicity. This phenomenon suggests that the hydrating mechanism that takes place during the hydrothermal sealing process is not as efficient

on modifying the surface properties as the Zr conversion coating; a possible explanation is that the mechanism of transition from alumina to bohemite and swelling of the pore walls does not provide the air trapping required to improve hydrophobicity, while the Zr nanocoating does it.

5 Conclusions

It was possible to propose a mechanism promoted by the treatment with H_2ZrF_6 on the anodized and bare AA7075 alloy, based on analyses of morphology, chemical composition and hydrophobicity. The F anions present in the solution activates the surface for the reaction of precipitation through a slight initial attack on the natural or porous anodic Al oxide, respectively for the bare and anodized alloy. A localized increase of pH takes place on these attacked regions, which allows the precipitation of Zr oxide. On the anodized alloy the mechanism also involves the growing of

Zr nanometric oxide towards the porous layer of the anodic oxide, indicating that the reaction happens not only on the pores' mouths but also along the superior portions of the pores' walls, i.e., inside the cavities. In addition, regions with cathodic intermetallic particles accumulated greater amounts of Zr oxide, due to its increased reactivity with the fluoride anions; this phenomenon was more noticeable for the bare alloy.

The contact angles indicated that nanometric properties of Zr oxide tend to produce hydrophobic surfaces on 7075-T6 aluminum alloy. However, a satisfactory effect was only ensured when this oxide is precipitated on the anodized alloy. Thus, one can suggest that the Zr nanometric oxide coating can act synergistically with the anodized layer of the AA7075-T6 alloy, creating a robust toxicity-free corrosion protection system. The greater increase on the contact angle provided by the Zr oxide over anodized samples can be mostly attributed to the nanometric scale of its porous layer,

suitable for obtaining hydrophobic surfaces, in contrast to the dense and compact natural aluminum oxide present on the bare alloy. Moreover, the Zr conversion coating brings a practical advantage over the hydrothermal sealing system, since it can be applied by immersion, for a few minutes and at room temperature.

Acknowledgements

The present work was carried out with support of CAPES and CNPq, which are Brazilian Governmental entities focused on providing resources for postgraduation and research. The authors are also thankful to Laboratory of Materials Corrosion, Protection and Recycle (LACOR) of Universidade Federal do Rio Grande do Sul (UFRGS) and the Materials Laboratory of Universidade Feevale.

References

- 1 Starke EAA Jr, Staley JT. Application of modern aluminum alloys to aircraft. *Progress in Aerospace Sciences*. 1996;32(2-3):131-172. [http://dx.doi.org/10.1016/0376-0421\(95\)00004-6](http://dx.doi.org/10.1016/0376-0421(95)00004-6).
- 2 Park JK, Ardell AJ. Microstructures of the commercial 7075 Al alloy in the T651 and T7 tempers. *Metallurgical Transactions. A, Physical Metallurgy and Materials Science*. 1983;14(10):1957-1965. <http://dx.doi.org/10.1007/BF02662363>.
- 3 Tian W, Li S, Wang B, Liu J, Yu M. Pitting corrosion of naturally aged AA 7075 aluminum alloys with bimodal grain size. *Evaluation and Program Planning*. 2016 [cited 2020 Nov 30];113:1-16. Available at: https://ac.els-cdn.com/S0010938X16307508/1-s2.0-S0010938X16307508-main.pdf?_tid=2468f932-c95d-11e7-9f71-00000aacb35e&acdnat=1510678934_a604a31ccc80e1f04153e94c61eec176
- 4 Harlow DG, Wei RP, Wang MZ. Statistical analysis of constituent particles in 7075-T6 aluminum alloy. *Metallurgical and Materials Transactions. A, Physical Metallurgy and Materials Science*. 2006;37(11):3367-3373. <http://dx.doi.org/10.1007/BF02586171>.
- 5 Pao PS, Feng CR, Gill SJ. Corrosion fatigue crack initiation in aluminum alloys 7075 and 7050. *Corrosion*. 2000;56(10):1022-1031. <http://dx.doi.org/10.5006/1.3294379>.
- 6 Zhao J, Xia L, Sehgal A, Lu D, McCreery RL, Frankel GS. Effects of chromate and chromate conversion coatings on corrosion of aluminum alloy 2024-T3. *Surface and Coatings Technology*. 2001;140(1):51-57. [http://dx.doi.org/10.1016/S0257-8972\(01\)01003-9](http://dx.doi.org/10.1016/S0257-8972(01)01003-9).
- 7 Santa Coloma P, Izagirre U, Belaustegi Y, Jorcín JBB, Cano FJJ, Lapeña N. Chromium-free conversion coatings based on inorganic salts (Zr/Ti/Mn/Mo) for aluminum alloys used in aircraft applications. *Applied Surface Science*. 2015;345:24-35. <http://dx.doi.org/10.1016/j.apsusc.2015.02.179>.
- 8 Golru SS, Attar MM, Ramezanzadeh B. Morphological analysis and corrosion performance of zirconium based conversion coating on the aluminum alloy 1050. *Journal of Industrial and Engineering Chemistry*. 2015;24:233-244. <http://dx.doi.org/10.1016/j.jiec.2014.09.036>.
- 9 García-Rubio M, De Lara MP, Ocón P, Diekhoff S, Beneke M, Lavía A, et al. Effect of posttreatment on the corrosion behaviour of tartaric-sulphuric anodic films. *Electrochimica Acta*. 2009;54(21):4789-4800. <http://dx.doi.org/10.1016/j.electacta.2009.03.083>.
- 10 Arenas MA, Conde A, De Damborenea JJ. Effect of acid traces on hydrothermal sealing of anodising layers on 2024 aluminium alloy. *Electrochimica Acta*. 2010;55(28):8704-8708. <http://dx.doi.org/10.1016/j.electacta.2010.07.089>.
- 11 García-Rubio M, Ocón P, Curioni M, Thompson GE, Skeldon P, Lavía A, et al. Degradation of the corrosion resistance of anodic oxide films through immersion in the anodising electrolyte. *Corrosion Science*. 2010;52(7):2219-2227. <http://dx.doi.org/10.1016/j.corsci.2010.03.004>.

- 12 Gonzalez JA, Lopez V, Otero E, Bautista A, Lizarbe R, Barba C, et al. Overaging of sealed and unsealed aluminium oxide films. *Corrosion Science*. 1997;39(6):1109-1118. [http://dx.doi.org/10.1016/S0010-938X\(97\)00019-X](http://dx.doi.org/10.1016/S0010-938X(97)00019-X).
- 13 O'Sullivan JP, Wood GC. The morphology and mechanism of formation of porous anodic films on aluminium. *Proceedings of the Royal Society A: Mathematical, Physical and Engineering Sciences*. 1970 [cited 2020 Nov 30];317(1531):511-543. Available at: <http://rspa.royalsocietypublishing.org/cgi/doi/10.1098/rspa.1970.0129>
- 14 Diggle JW, Downie TC, Goulding CW. Anodic oxide films on aluminum. *Chemical Reviews*. 1969;69(3):365-405. <http://dx.doi.org/10.1021/cr60259a005>.
- 15 Hu N, Dong X, He X, Browning JF, Schaefer DW. Effect of sealing on the morphology of anodized aluminum oxide. *Corrosion Science*. 2015;97:17-24. <http://dx.doi.org/10.1016/j.corsci.2015.03.021>.
- 16 Mauricio O, Ramirez P, Donatus U, Queiroz FM, Olivier MG, Costa I, et al. EIS investigation of a Ce - based posttreatment step on the corrosion behaviour of Alclad AA2024 anodized in TSA. *Surface and Interface Analysis*. 2019;51:1260-1275.
- 17 Wang R, Wang L, He C, Lu M, Sun L. Studies on the sealing processes of corrosion resistant coatings formed on 2024 aluminium alloy with tartaric-sulfuric anodizing. *Surface and Coatings Technology*. 2019;360:369-375. <http://dx.doi.org/10.1016/j.surfcoat.2018.12.092>.
- 18 Costenaro H, Lanzutti A, Paint Y, Fedrizzi L, Terada M, Melo HG, et al. Corrosion resistance of 2524 Al alloy anodized in tartaric-sulphuric acid at different voltages and protected with a TEOS-GPTMS hybrid sol-gel coating. *Surface and Coatings Technology*. 2017;324:438-450. <http://dx.doi.org/10.1016/j.surfcoat.2017.05.090>.
- 19 Guadagnin HC. Corrosion resistance study of AA2524 anodized in sulphuric-tartaric acid and sealed with hybrid coatings [thesis]. São Paulo: Universidade de São Paulo; 2017 [cited 2018 Dec 8]. Available at: <http://www.teses.usp.br/teses/disponiveis/3/3137/tde-20072017-152947/>
- 20 Terada M, Queiroz FM, Aguiar DBS, Ayusso VH, Costenaro H, Olivier M, et al. Corrosion resistance of tartaric-sulfuric acid anodized AA2024-T3 sealed with Ce and protected with hybrid sol-gel coating. *Surface and Coatings Technology*. 2019;372:422-426. <http://dx.doi.org/10.1016/j.surfcoat.2019.05.028>.
- 21 Pinheiro JS, Regio G, Cardoso HRP, Oliveira CT, Ferreira JZ. Influence of concentration and ph of hexafluorozirconic acid on corrosion resistance of anodized AA7075-T6. *Materials Research*. 2019;22(Supplement 1):e20190048. <http://dx.doi.org/10.1590/1980-5373-mr-2019-0048>.
- 22 Yu S, Wang L, Wu C, Feng T, Cheng Y, Bu Z, et al. Studies on the corrosion performance of an effective and novel sealing anodic oxide coating. *Journal of Alloys and Compounds*. 2020;817:153257. <http://dx.doi.org/10.1016/j.jallcom.2019.153257>.
- 23 Saenz de Miera M, Curioni M, Skeldon P, Thompson GE. The behaviour of second phase particles during anodizing of aluminium alloys. *Corrosion Science*. 2010;52(7):2489-2497. <http://dx.doi.org/10.1016/j.corsci.2010.03.029>.
- 24 Ma Y, Zhou X, Thompson GE, Curioni M, Hashimoto T, Skeldon P, et al. Anodic film formation on AA 2099-T8 aluminum alloy in tartaric-sulfuric acid. *Journal of the Electrochemical Society*. 2011;158(2):C17. <http://dx.doi.org/10.1149/1.3523262>.
- 25 Huang Y-S, Shih T-S, Chou J-H. Electrochemical behavior of anodized AA7075-T73 alloys as affected by the matrix structure. *Applied Surface Science*. 2013;283:249-257. <http://dx.doi.org/10.1016/j.apsusc.2013.06.094>.
- 26 Ma Y, Zhou X, Thompson GE, Curioni M, Skeldon P, Zhang X, et al. Anodic film growth on Al-Li-Cu alloy AA2099-T8. *Electrochimica Acta*. 2012;80:148-159. <http://dx.doi.org/10.1016/j.electacta.2012.06.126>.
- 27 Ma Y, Wu H, Zhou X, Li K, Liao Y, Liang Z, et al. Corrosion behavior of anodized Al-Cu-Li alloy: the role of intermetallic particle-introduced film defects. *Corrosion Science*. 2019;158:108110. <http://dx.doi.org/10.1016/j.corsci.2019.108110>.
- 28 Capelossi VR, Poelman M, Recloux I, Hernandez RPB, Melo HG, Olivier MG. Corrosion protection of clad 2024 aluminum alloy anodized in tartaric-sulfuric acid bath and protected with hybrid sol-gel coating. *Electrochimica Acta*. 2014;124:69-79. <http://dx.doi.org/10.1016/j.electacta.2013.09.004>.
- 29 Runge JM. *The metallurgy of anodizing aluminum*. Cham: Springer International Publishing; 2018. <http://dx.doi.org/10.1007/978-3-319-72177-4>.
- 30 Hitzig J, Jüttner K, Lorenz WJJ, Paatsch W. AC-impedance measurements on porous aluminium oxide films. *Corrosion Science*. 1984;24(11-12):945-952. [http://dx.doi.org/10.1016/0010-938X\(84\)90115-X](http://dx.doi.org/10.1016/0010-938X(84)90115-X).
- 31 Lunder O. Chromate-free pre-treatment of aluminium for adhesive bonding [thesis]. Trondheim: Fakultet for Naturvitenskap og Teknologi; 2003.

- 32 Andreatta F, Turco A, de Graeve I, Terryn H, de Wit JHW, Fedrizzi L. SKPFM and SEM study of the deposition mechanism of Zr/Ti based pre-treatment on AA6016 aluminum alloy. *Surface and Coatings Technology*. 2007;201(18):7668-7685. <http://dx.doi.org/10.1016/j.surfcoat.2007.02.039>.
- 33 Li L, Desouza AL, Swain GM. In situ pH measurement during the formation of conversion coatings on an aluminum alloy (AA2024). *Analyst*. 2013;138(15):4398-4402. <http://dx.doi.org/10.1039/c3an00663h>.
- 34 Li L, Whitman BW, Swain GM. Characterization and Performance of a Zr/Ti Pretreatment Conversion Coating on AA2024-T3. *Journal of the Electrochemical Society*. 2015;162(6):C279-C284. <http://dx.doi.org/10.1149/2.0901506jes>.
- 35 García-Rubio M, De Lara MP, Ocón P, Diekhoff S, Beneke M, Lavía A, et al. Effect of posttreatment on the corrosion behaviour of tartaric-sulphuric anodic films. *Electrochimica Acta*. 2009;54(21):4789-4800. <http://dx.doi.org/10.1016/j.electacta.2009.03.083>.
- 36 Boisier G, Pébère N, Druetz C, Villatte M, Suel S, Fesem SS, et al. FESEM and EIS study of sealed AA2024 T3 anodized in sulfuric acid electrolytes: influence of tartaric acid. *Journal of the Electrochemical Society*. 2008;155(11):521-529. <http://dx.doi.org/10.1149/1.2969277>.
- 37 Salles Pinheiro J, Zoppas Ferreira J. Proteção da liga AA7075-T6 por anodização tartárico-sulfúrica e pós-tratamento com ácido hexafluorozircônico [dissertation]. Porto Alegre: Universidade Federal do Rio Grande do Sul; 2019.
- 38 George FO, Skeldon P, Thompson GE. Formation of zirconium-based conversion coatings on aluminium and Al-Cu alloys. *Corrosion Science*. 2012;65:231-237. <http://dx.doi.org/10.1016/j.corsci.2012.08.031>.
- 39 Liu T, Dong L, Liu T, Yin Y. Investigations on reducing microbiologically-influenced corrosion of aluminum by using super-hydrophobic surfaces. *Electrochimica Acta*. 2010;55(18):5281-5285. <http://dx.doi.org/10.1016/j.electacta.2010.04.082>.
- 40 Thangavelu A, Sukumaran A, Hariprasad S, Gowtham S, Ravisankar B, Krishna LR, et al. Fabrication of corrosion resistant hydrophobic ceramic nanocomposite coatings on PEO treated AA7075. *Ceramics International*. 2018;44(1):874-884. <http://dx.doi.org/10.1016/j.ceramint.2017.10.014>.
- 41 Li Y, Li S, Zhang Y, Yu M, Liu J. Fabrication of superhydrophobic layered double hydroxides films with different metal cations on anodized aluminum 2198 alloy. *Materials Letters*. 2015;142:137-140. <http://dx.doi.org/10.1016/j.matlet.2014.11.148>.
- 42 Wenzel RN. Resistance of solid surfaces to wetting by water. *Industrial & Engineering Chemistry*. 1936;28(8):988-994. <http://dx.doi.org/10.1021/ie50320a024>.
- 43 Cassie BD, Baxter S. Wettability of porous surfaces. *Transactions of the Faraday Society*. 1944;40(5):546-551. <http://dx.doi.org/10.1039/TF9444000546>.
- 44 Verplanck N, Coffinier Y, Thomy V, Boukherroub R. Wettability switching techniques on superhydrophobic surfaces. *Nanoscale Research Letters*. 2007;2(12):577-596. <http://dx.doi.org/10.1007/s11671-007-9102-4>.
- 45 Niu JJ, Wang JN. A novel self-cleaning coating with silicon carbide nanowires. Washington: ACS Publications; 2020 [cited 2020 Nov 20]; Available at: <https://pubs.acs.org/sharingguidelines>

Received: 30 June 2020

Accepted: 4 Dec. 2020